

Understanding Digestive Ripening of Ligand-Stabilized, Charged Metal Nanoparticles

José A. Manzanares,^{a,} Pekka Peljo^b and Hubert H. Girault^b*

^aDepartment of Thermodynamics, Faculty of Physics, University of Valencia, c/Dr. Moliner, 50, E-46100 Burjasot, Spain

^bLaboratoire d'Electrochimie Physique et Analytique, École Polytechnique Fédérale de Lausanne, EPFL Valais Wallis, Rue de l'Industrie 17, Case Postale 440, CH-1951 Sion, Switzerland

SUPPORTING INFORMATION

Ligand packing density on Au NPs. The number of bound ligands on a NP of radius r_n is $L_n \approx L_1 n^{2/3}$, where $L_1 \equiv 4\pi / (\kappa^2 A_L)$, $\kappa \equiv (4\pi / 3V_M)^{1/3}$, and V_M is the volume per metal atom in the NP; i.e. $A_n \approx L_n A_L \approx 4\pi r_n^2$ is the total NP surface area. The self-assembled monolayers of dodecanethiol on Au(111) surfaces have an area per ligand^{5,7,10,57,61} $A_L = 0.214 - 0.216 \text{ nm}^2$ (equivalent to a thiolate packing density of 4.63 nm^{-2}), which corresponds to three gold surface atoms per thiolate adsorbate. In the case of Au NPs, the number of surface atoms per thiolate is lower. Gelbart et al. suggested using the same value of A_L for Au(111) and Au NPs, because the lower number of surface atoms per thiolate could be explained by curvature effects, e.g. to 2.3 Au:thiolate for 1.0 nm radius NPs.⁷ However, experimental results and MD simulations suggest a greater packing density on NPs so that the actual ratio of surface atoms to thiolate is ca. 1.6 for 1.0 nm radius Au NPs. Thus, a range $A_L = 0.15 - 0.17 \text{ nm}^2$ seems justified for very small NPs.^{46,62-64} A recent study on the effect of the ligand chain length ℓ (in nm) on their packing density on Au NPs concluded that L_n has a linear dependence with ℓ , $1/A_L = (6.7453 - 0.6997\ell) \text{ nm}^{-2}$;⁵⁷ that is, slightly higher coverages of Au NPs can be achieved using short-chain ligands. This expression predicts $A_L \approx 0.18 \text{ nm}^2$ for $\ell \approx 1.8$, the estimated chain length in nm of dodecanethiol. In this work, the coefficient L_1 has been obtained by fitting the literature data^{19,35,39,44,63-67} on the number of adsorbed thiolates as a function of the number of gold atoms to the expression $L_n = L_1 n^{2/3}$, with the result $L_1 = 1.810 \pm 0.012$ and $A_L = 4\pi / (\kappa^2 L_1) = 0.1764 \pm 0.0012 \text{ nm}^2$. This value of A_L accurately describes a wide range of NP sizes (Figure S1) and is very close to those used in the literature.^{62-64,68} However, the

functional dependence $L_n = L_1 n^{2/3}$ is so simple that experimental data for nanoclusters and very small NPs (with less than 100 ligands) show some minor deviations (Figure S1 inset).

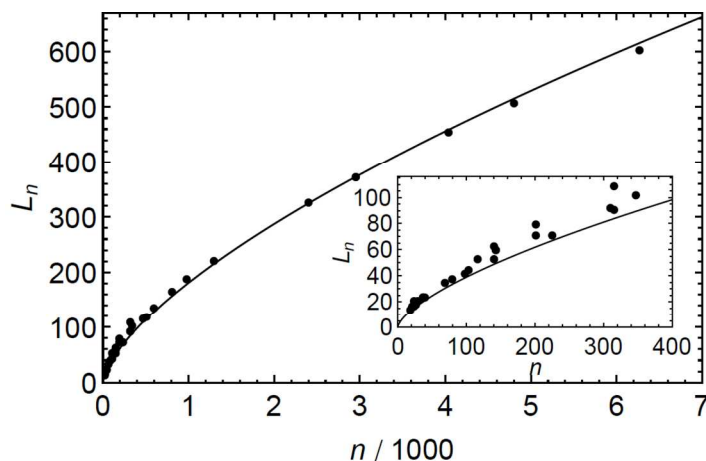


Figure S1. Determination of the effective area per ligand A_L . The solid line is the fit of the experimental data on alkanethiolate-Au NPs to $L_n = L_1 n^{2/3}$.

Surface energy and size dependence of the surface tension of Au NPs. The contribution of the surface free energy to the chemical potential of the NPs is given by $\mu_n^{\text{surf}} = \gamma_n A_n$, which simplifies to $\mu_n^{\text{surf}} = \gamma_\infty 4\pi r_n^2$ in the case of very large NPs. MD simulations data⁴⁵ can be accurately fitted to $\mu_n^{\text{surf}} = \gamma_n A_n = a n^{2/3}$ with $a = 1.8765 \pm 0.0085$ eV (Figure S2). The parameter $a = 4\pi\gamma_\infty / \kappa^2$ corresponds to a surface free energy $\gamma_\infty = 0.980$ J/m², in agreement with experimental observations.⁴⁵ The expression $\gamma_n A_n \approx a n^{2/3}$ does not imply that $A_n \propto n^{2/3}$ and that γ_n is size independent. On the contrary, the MD simulations evidence that γ_n increases with decreasing NP size because of the associated increase in the fraction of edge and corner sites.⁴⁵

However, this effect is partly compensated by the fact that A_n has other size-dependent contributions in addition to the leading term $\propto n^{2/3}$, and hence $\gamma_n A_n \approx an^{2/3}$ turns out to be a simple yet accurate expression.

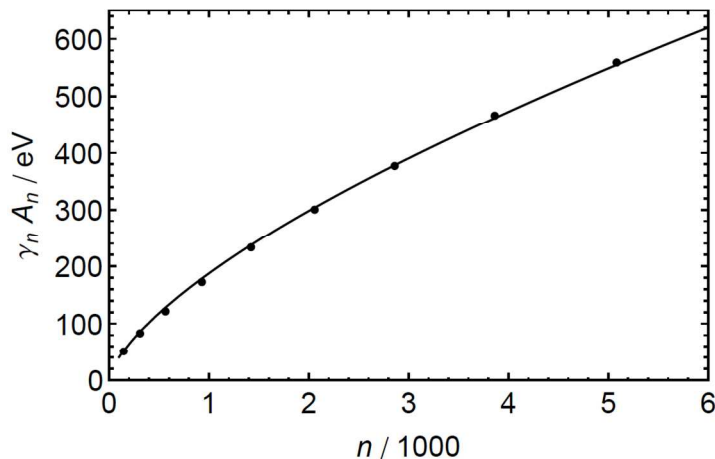


Figure S2. Surface contribution (from MD simulations⁴⁵) to the chemical potential of NPs estimated as the difference between the potential energy of an icosahedral NP and that of a bulk system containing the same number n of atoms.

A large number of theoretical and experimental studies have established that the interfacial free energy γ_n of nanocrystals is size dependent. Although the Tolman equation

$$\gamma_n = \gamma_\infty / (1 + 2\delta / r_n)$$

is often cited,⁴⁰ its validity has been questioned for very small NPs.^{69,70}

Moreover, in addition to the seminal contributions by Tolman, Guggenheim, and Kirkwood and Buff that predict a positive Tolman length δ , another rigorous derivation⁷¹ predicts negative δ .

With special focus on nanocrystals, studies concluding both the decrease⁷² and the increase⁴⁵ of interfacial free energy with decreasing size can be found. To the best of our understanding, these apparently contradictory results simply reflect two different conventions. When the surface

atoms are compared to those in the NP core, a decrease in the NP size reduces their energy difference,⁷⁰ and hence $\delta > 0$. However, when the surface atoms are compared to those in bulk metal, a decrease in NP size increases their energy difference⁴⁵ and hence $\delta < 0$. In our theoretical model the bulk metal has been chosen as the standard state of the metal atoms.

Consistently, we have evaluated $\mu_n^{\text{surf}} = \gamma_n A_n$ from surface free energy calculated with respect to the bulk metal (Figure S2).

Finally, it is reasonable to neglect the facet effects because the values reported for the interfacial free energy of Au NPs may differ by up to several J/m^2 ,⁷³ while the difference between γ_∞ for bulk Au(111) and bulk Au(100) is only about $0.1 - 0.3 \text{ J/m}^2$.⁴⁵

Alkanethiol binding energy on Au NPs. The sulfur head of alkanethiols strongly binds to Au substrates and forms a metal thiolate. Although the monolayers of alkanethiols on both Au NPs and Au(111) substrates have been intensively studied, both in experiments and computations, there remain many uncertainties in the binding energies.⁷⁴ The theory of ligand-stabilized metal NPs developed by Gelbart, Heath and coworkers estimated this chemisorption binding energy as 1.0 eV .⁷ Lavrick et al. estimated the chemisorption enthalpy of alkanethiols on Au(111) as 126 kJ/mol (equivalent to 1.31 eV per sulphur head) independently of the alkyl chain length.⁷⁵ However, other experimental results on planar substrates have lead to estimate the alkanethiol-gold binding energy as^{64,76} 1.91 eV or within the range $1.7 - 2.1 \text{ eV}$.⁴⁴ Moreover, while sulphur sits on three gold atoms when chemisorbed on planar Au(111), it sits on a lower number of gold atoms on NPs (ca. 1.6 for 2.0 nm diameter⁶³) and it must definitively affect the binding energy. Thus, using atomistic MD with a force field optimized from DFT calculations, Heath and

coworkers estimated the binding energy of ethanethiol on a Au₃₂ nanocluster as 1.06 eV.⁷⁴ The value 1.6 eV for the binding energy of thiolate on Au NPs that we have used seems quite reasonable for the range of NP sizes observed after the DR process because it is intermediate between the experimental estimates of 1.31 eV and 1.91 eV.

The binding energies of different capping ligands have been estimated from DFT calculations.⁵⁶ Thus, accepting the value^{63,76} 184.1 kJ/mol (1.91 eV) as an upper estimate for the binding energy of butanethiol on planar substrates, the binding energies of trimethylphosphine, butylamine, and buthyl thiocyanate can be estimated as 81.7 kJ/mol (0.85 eV), 58.8 kJ/mol (0.61 eV), and 28.8 kJ/mol (0.30 eV), respectively. When used to estimate ligand binding to NPs, these energies should be reduced by a factor of ca. 0.8 to take into account that the bonds are weaker when the head interacts with a lower number of metal atoms due to the NP curvature. In any case, these values reflect that the covalent bond in gold-thiolate is more stable than dative bond in gold-phosphine and amine.⁷⁷

SUPPLEMENTARY REFERENCES

61. Nuzzo, R. G.; Zegarski, B. R.; Dubois, L. H. Fundamental Studies of the Chemisorption of Organosulfur Compounds on Au(111). Implications for Molecular Self-Assembly on Gold Surfaces. *J. Am. Chem. Soc.* **1987**, *109*, 733–740.
62. Badia, A.; Singh, S.; Demers, L.; Cuccia, L.; Brown, G. R.; Lennox, R. B. Self-Assembled Monolayers on Gold Nanoparticles. *Chem. Eur. J.* **1996**, *2*, 359–363.
63. Badia, A.; Cuccia, L.; Demers, L.; Morin, F.; Lennox, R. B. Structure and Dynamics in Alkanethiolate Monolayers Self-Assembled on Gold Nanoparticles: A DSC, FT-IR, and Deuterium NMR Study. *J. Am. Chem. Soc.* **1997**, *119*, 2682–2692.

64. Luedtke, W. D.; Landman, U. Structure and Thermodynamics of Self-Assembled Monolayers on Gold Nanocrystallites. *J. Phys. Chem. B* **1998**, *102*, 6566–6572.
65. Daniel, M.-C.; Astruc, D. Gold Nanoparticles: Assembly, Supramolecular Chemistry, Quantum-Size-Related Properties, and Applications toward Biology, Catalysis, and Nanotechnology. *Chem. Rev.* **2004**, *104*, 293–346.
66. Jadzinsky, P. D.; Calero, G.; Ackerson, C. J.; Bushnell, D. A.; Kornberg, R. G. Structure of a Thiol Monolayer–Protected Gold Nanoparticle at 1.1 Å Resolution. *Science* **2007**, *318*, 430–433.
67. Hostetler, M. J.; Templeton, A. C.; Murray, R. W. Dynamics of Place-Exchange Reactions on Monolayer-Protected Gold Cluster Molecules. *Langmuir* **1999**, *15*, 3782–3789.
68. Pradeep, T.; Sandhyarani, N. Structure and Dynamics of Monolayers on Planar and Cluster Surfaces. *Pure Appl. Chem.* **2002**, *74*, 1593–1607.
69. Nanda, K. K.; Maisels, A.; Kruis, F. E.; Fissan, H.; Stappert, S. Higher Surface Energy of Free Nanoparticles. *Phys. Rev. Lett.* **2003**, *91*, 106102.
70. Lu, H. M.; Jiang, Q. Size-Dependent Surface Tension and Tolman’s Length of Droplets. *Langmuir* **2005**, *21*, 779–781.
71. van Giessen, A. E.; Blokhuis, E. M.; Bukman, D. J. Mean Field Curvature Corrections to the Surface Tension. *J. Chem. Phys.* **1998**, *108*, 1148–1154.
72. Ouyang, G.; Tan, X.; Yang, G. Thermodynamic Model of the Surface Energy of Nanocrystals. *Phys. Rev. B* **2006**, *74*, 195408.
73. Nanda, K. K.; Maisels, A.; Kruis, F. E. Surface Tension and Sintering of Free Gold Nanoparticles. *J. Phys. Chem. C* **2008**, *112*, 13488–13491.
74. Jang, S. S.; Jang, Y. H.; Kim, Y.-H.; Goddard III, W. A.; Flood, A. H.; Laursen, B. W.; Tseng, H.-R.; Stoddart, J. F.; Jeppesen, J. O.; Choi, J. W.; Steuerman, D. W.; DeIonno, E.; Heath, J. R. Structures and Properties of Self-Assembled Monolayers of Bistable

- [2]Rotaxanes on Au (111) Surfaces from Molecular Dynamics Simulations Validated with Experiment. *J. Am. Chem. Soc.* **2005**, *127*, 1563–1575.
75. Lavrich, D. J.; Wetterer, S. M.; Bernasek, S. L.; Scoles, G. Physisorption and Chemisorption of Alkanethiols and Alkyl Sulfides on Au(111). *J. Phys. Chem. B* **1998**, *102*, 3456–3465.
76. Dubois, L. H.; Nuzzo, R. G. Synthesis, Structure, and Properties of Model Organic Surfaces. *Annu. Rev. Phys. Chem.* **1992**, *43*, 437–463.
77. Jin, R.; Zeng, C.; Zhou, M.; Chen, Y. Atomically Precise Colloidal Metal Nanoclusters and Nanoparticles: Fundamentals and Opportunities. *Chem Rev.* **2016**, *116*, 10346–10413.